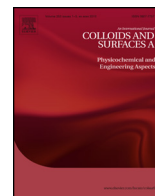




Contents lists available at ScienceDirect

Colloids and Surfaces A: Physicochemical and Engineering Aspects

journal homepage: www.elsevier.com/locate/colsurfa

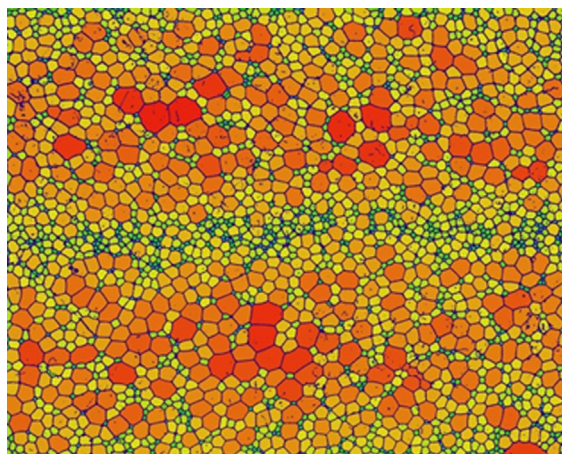
Foam stability in the presence and absence of hydrocarbons: From bubble- to bulk-scale

Kofi Osei-Bonsu^a, Nima Shokri^{a,*}, Paul Grassia^{b,c}^a School of Chemical Engineering and Analytical Science, University of Manchester, Manchester M13 9PL, UK^b Department of Chemical and Process Engineering, University of Strathclyde, James Weir Building, 75 Montrose St, Glasgow G1 1XJ, UK^c Ciencias Matemáticas y Físicas, Universidad Católica de Temuco, Rudecindo Ortega 02950, Temuco, Chile

HIGHLIGHTS

- Foam stability was investigated at both bulk- and bubble-scale.
- Effects of type of oil and surfactant on foam stability was investigated.
- Our results illustrated less stable foam in the presence of oil.
- Adverse impact on foam stability was reduced as oil viscosity and density increased.
- Presence of oil increases coarsening rate of foams deduced from the bubble-scale visualization.

GRAPHICAL ABSTRACT



ARTICLE INFO

Article history:

Received 15 May 2015

Received in revised form 9 June 2015

Accepted 10 June 2015

Available online 15 June 2015

Keywords:

Foam stability

Foam-oil interaction

Surfactant

Bubble-scale visualization

Oil effects on

foam stability

ABSTRACT

One of the pioneering applications of foam is in enhanced oil recovery (EOR). A major stumbling-block to the success of foam application in EOR is the adverse influence of oil on foam stability. The objectives of the present work were to evaluate the effects of various surfactants and hydrocarbons with well-defined properties on foam stability. To do so, we have conducted a comprehensive series of experiments at bulk- and bubble-scale to investigate the foam stability of four surfactants in the absence and presence of three isoparaffins distinguished by their carbon chain length, density and viscosity. For the bulk foam stability experiments, foam was generated by sparging pure air into surfactant solution in a vertical cylindrical column. An automated camera was used to record the gradual decay of foam as a function of time. The results showed the significant impact of the type of the surfactant on foam stability. Besides, our results illustrated less stable foam in the presence of oil with less adverse impact on foam stability as oil viscosity and density increased. The limitation of the method used in the present study to quantify foam stability, i.e., measuring the decay of foam height over a certain period of time, which is a commonly used method in literature, is discussed here and an alternative approach is proposed to investigate foam stability at bubble-scale to supplement and improve understanding of the physical phenomena controlling foam stability.

© 2015 The Authors. Published by Elsevier B.V. This is an open access article under the CC BY license (<http://creativecommons.org/licenses/by/4.0/>).

* Corresponding author at: School of Chemical Engineering and Analytical Science Room C26, The Mill, The University of Manchester Sackville Street, Manchester M13 9PL, UK.

E-mail address: nima.shokri@manchester.ac.uk (N. Shokri).

URL: <http://personalpages.manchester.ac.uk/staff/nima.shokri/> (N. Shokri).

<http://dx.doi.org/10.1016/j.colsurfa.2015.06.023>

0927-7757/© 2015 The Authors. Published by Elsevier B.V. This is an open access article under the CC BY license (<http://creativecommons.org/licenses/by/4.0/>).

1. Introduction

It is common in petroleum exploitation to inject water into reservoirs to drive out reservoir fluids as well as to maintain the reservoir pressure as the natural pressure of the reservoir declines over the course of production. Typically, about 65% of hydrocarbons remain unproduced after natural drive and water flooding [1,2]. This remaining oil is a target for enhanced oil recovery (EOR) methods such as gas injection and chemical EOR. Though gas recovery methods such as carbon dioxide and steam injection have shown potential to improve oil recovery, the major shortcomings of these EOR methods are their poor volumetric sweep efficiency (due to poor gas contact with oil) [3,4]. This occurs primarily because of reservoir heterogeneity and also the density and viscosity contrast between the injected gas and the reservoir fluids. Injected gas tends to flow preferentially through high permeability streaks (channelling) while viscosity and density differences result in viscous fingering and gravity override respectively [5–7].

Displacement by foam has proven to be a potential remedy to these complications, improving the efficiency of oil production [8–10]. Foam can be defined as a dispersion of gas in a liquid such that the liquid phase is continuous with some of the gas trapped in thin liquid films called lamellae [11]. The suitability of foam for EOR is due to its ability to reduce gas relative permeability by trapping gas bubbles in porous media [12]. The presence of bubbles increases the gas effective viscosity, which provides stability in the displacement process [13–17]. Foam also improves sweep by reducing gas mobility in high permeability areas thereby allowing diverted gas to sweep hydrocarbons in low permeability areas [12]. It has also been suggested that the presence of some surfactants in foam reduces capillary forces through reduction of interfacial tension between the displacing and displaced fluid [18].

The stability of foams is crucial to effective oil displacement. Foam stability is controlled by many factors associated with the physiochemical properties of the surfactant solution such as surface tension, surface viscosity and elasticity amongst others (see [19] for comprehensive information about the factors affecting foam stability). Among these factors is a parameter of paramount importance known as the disjoining pressure Π . The disjoining pressure is essentially the total pressure difference between the gas phase and the liquid phase within a film and it is highly dependent on the film thickness [19]. As described by the DLVO theory [20,21], contributions to disjoining forces arise fundamentally from two main sources: repulsive positive electrostatic potentials and attractive negative van der Waals potentials. The attractive van der Waals component results from the dipole-induced-dipole interactions between molecules across the film. These forces dominate where surfactant is absent making disjoining pressure negative and hence lamellae short lived. Upon the introduction of surfactant, the surfactant molecules adsorb onto the gas liquid interface. Surfactant adsorption results in an electrical double-layer which is the source of the repulsive force that stabilizes the lamellae. As a result, one of the parameters amongst others that define the degree of stabilization is the ionic strength of the aqueous solution [9].

One of the major challenges to the success of foam in EOR is the adverse influence of oil on foam stability and also characterisation of the complex interaction between foam and oil [14,22]. Results from bulk foam experiments in the literature show an apparent contradiction of the effect of oil on foam stability. Some authors have argued that the presence of oil, especially lighter hydrocarbons, destroy or prevent the generation of foam [23–25]. Others, however, have shown that stable foams can be generated in the presence of oil if an appropriate foaming agent is selected [22,26,27]. It has also been demonstrated that foam can be gener-

ated effectively in the presence of heavy oil [28,29]. Indeed, there are other experiments that suggest that oil can improve the stability of foam. For example, Aveyard et al. [30] conducted a series of experiments to delineate the correlation between alkanes and the half-life of a single foam bubble. While their results confirmed that lighter chain hydrocarbons radically reduce the longevity of foams, they also observed that longer chain hydrocarbons increased foam stability. Furthermore, Koczo et al. [31] have shown that emulsified oil can enhance the longevity of foams if the pseudoemulsion film is stable.

The destabilizing effects of oil on foam are believed to be a result of direct surface interactions between oil and foam which are determined by various physiochemical properties [14]. It is widely accepted that these interactions are governed by three main mechanisms; entry of oil droplet into gas-liquid interface [32,33], spreading of oil on the gas-liquid interface [34], and formation of an unstable bridge across lamella [35]. As discussed in Schramm and Novosad [24] the thermodynamic feasibility of oil destroying foam can be determined by evaluating the entering coefficient (E), spreading coefficient (S) and bridging coefficient (B). The mathematical expressions for E , S and B are given by

$$E = \sigma_{wg} + \sigma_{ow} + \sigma_{og} \quad (1)$$

$$S = \sigma_{wg} + \sigma_{ow} + \sigma_{og} \quad (2)$$

$$B = \sigma_{wg}^2 + \sigma_{ow}^2 + \sigma_{og}^2 \quad (3)$$

where σ_{wg} is the surface tension between surfactant solution and the gas, σ_{ow} is the interfacial tension between oil and surfactant solution and σ_{og} is the surface tension between the oil and gas.

The first condition to be satisfied for oil to destroy foam is that the oil droplet must be able to invade the gas–water interface [30]. This condition is met when $E > 0$ [33]. It is worth noting that, entering is not possible until oil is present in the form of emulsified oil, i.e., droplets with the droplet sizes smaller than the thickness of the foam lamella [24]. Once oil droplet has entered the gas-liquid interface, it will spread on the surface of the film. This occurs when $S > 0$ [32]. The spreading of the oil droplet over the film interface forces liquid out of the film into the Plateau borders which causes the film to thin and eventually rupture. Also, it has been suggested that the spreading of oil alters the film interfacial rheology which could change the rate of film drainage [36]. Ewers and Sutherland [37] suggested that both the entry and spreading condition must be satisfied for oil droplet to act as antifoam. On the contrary, when $S < 0$ (no oil spreading), oil forms a lens at the interface between the gas and liquid and may eventually destroy foam film if it makes its way into the lamella surface (bridging mechanism where $B \geq 0$) [30,38]. In fact, Vikingstad et al. [39] conducted a systematic static bulk foam test to investigate the factors that affect foam stability. Their results showed that negative spreading coefficient is not prerequisite for stable foam formation.

Mannhardt et al. [26] found that the stability of foams is related to the stability of pseudoemulsion films. When the pseudoemulsion film formed between the oil droplet and gas phase is stable, oil spreading is suppressed. Oil will only spread or bridge gas-liquid interface when the pseudoemulsion film ruptures. Manlowe and Radke [40] observed this mechanism in their pore-scale investigation of foam-oil interaction. They likewise concluded that the stability of foams is dependent on the stability of pseudoemulsion films and they did not find any relationship between oil spreading and foam stability. Similarly Koczo et al. [31] found that the entering and spreading coefficient had no correlation with the stability of foam as the pseudoemulsion film must rupture before oil can enter or spread in the air–water interface. Hadjiiski et al. [41] demonstrated from their experimental study the role of this ‘entry barrier’ in the destruction of foam by oil. They developed a novel

Table 1
Properties of surfactant solutions (2% concentration) used in our experiments to investigate foam stability. Each of the solutions was stirred for 30 min before the surface tensions were measured (at room temperature).

Surfactant solution	Active content (%)	Charge	Surface tension (mN m ⁻¹)
Sodium dodecyl sulphate (SDS)	85	Anionic	28.76
Trixton X100	100	Non-ionic	29.95
Cocamidopropyl betaine	30.7	Zwitterionic	29.93

method to measure the critical capillary pressure associated with entry of an oil drop into foam. Their results showed a direct correlation between the critical capillary pressure and the final height of foam.

It has been observed that mixing surfactants can significantly improve the stability of foams and potentially reduce the destabilizing effect of oil on foam [28,42]. For example addition of small fractions of non-ionic surfactant to an anionic surfactant enhances the foam stability as a result of the formation of a viscous surface layer which raises the interfacial viscosity of the foam thereby reducing the rate of film thinning [19]. Betaines are known for their foam enhancing properties [14]. In their 2D sand-pack experiments, Li et al. [42] observed that the addition of lauryl betaine to the so called NI blend (4:1 of Neodol 67-7PO sulfate and IOS 15–18) generated a stronger and more stable foam in the presence of oil. One of the mechanisms suggested for this stabilising behavior is that betaine increases the critical capillary pressure required for droplet entry which is related to the disjoining pressure [14,43].

Notwithstanding the success in applying foam in oil recovery both in laboratory [18,28] and in field tests [44,45], there still remain challenges in the understanding of foam stability for a given surfactant, oil and boundary condition. Motivated by the importance of foam stability in various applications including oil recovery, the specific objectives of the present work are to study systematically the stability of foams and the effects of oil properties (i.e., viscosity and density) on foam stability at bulk- and bubble-scale. In most of the previous studies [28,39,46,47], foam stability was investigated by monitoring the changes in the height of bulk foam in vertical columns over time. Although this type of experimental setup provides valuable information about the effects of several parameters such as surfactant concentrations and type of oil and surfactant on the foam stability, it provides limited information about the bubble-scale dynamics as the measurement is mainly conducted at bulk-scale. Inferences regarding foam coarsening and coalescence rate are merely qualitative. Bubble-scale information is required to understand fully the physics governing foam stability under a given set of conditions. There are many valuable works in the literature that deal with various aspects of foam dynamics at bubble scale (e.g., [48–51]) but few if any have attempted to evaluate and compare the stability of foams at bulk and bubble-scale. In this study we introduce a method to describe quantitatively the coarsening rate at the bubble scale (which is one of the factors that control liquid film thinning and dictates the foam stability at the bulk-scale). We also compare the foam stability at bulk-scale to the bubble-scale stability to understand the principal physical mechanisms causing decay or rupture in foams made with selected surfactant.

2. Experimental considerations

2.1. Material and methods

To investigate foam stability in the absence and presence of oil, we employed three surfactants in our experiments; cocamidopropyl betaine (Cocobetaine) (The Soap Kitchen, UK); sodium dodecyl sulphate (SDS) (Sigma, UK) and Triton X100 (Sigma, UK).

A fourth surfactant was created by mixing 1:1 ratio of Cocobetaine and SDS which is referred as CocoSDS hereafter. Two of the surfactants, Cocobetaine and Triton X100 were supplied in the liquid phase while SDS was received in powdered form. Surfactant solutions of 2% concentration (active content) were prepared with 0.5 M NaCl (Sigma, UK) in deionised water (18.2 MΩ/cm). The properties of surfactant solutions are listed in Table 1. The viscosities of the surfactant solutions are presented in Appendix A (the viscosities were measured by a rheometer – TA Instruments AR2000). These surfactants were chosen based on their charges (reported in Table 1). Three isoparaffins were used as the oil phase namely, Isopar G, Isopar N and Isopar V (Brenntag, UK). These oils belong to the same isoparaffin series and are distinguished by their density, viscosity and surface tension as given in Table 2 enabling us to investigate the effects of oil viscosity and density on foam stability. The surface tensions of the surfactant solutions and the oils were measured by a tensiometer (Kruss, Germany) at 25 °C following the du Nouy ring method [52]. The interfacial tensions were also measured with a spinning drop tensiometer (Krüss SITE 04, Germany).

2.2. Bulk-scale foam stability

We designed and developed an experimental setup to quantify the bulk foam height as a function of time for determining foam stability at bulk-scale as shown in Fig. 1(a).

For the bulk-scale experiment, a chromatography column (Scientific Glass, UK) with an inner diameter and height of 4 cm and 80 cm, respectively was used. Fitted to the bottom was a sintered glass disk with a pore size distribution of 40–100 μ. The function of the sintered glass was to enable gas sparging. In this study, air was used to make foam which was injected into column containing 100 cm³ of the surfactant solution at a volumetric flux of 100 cm³/min (±0.1 cm³/min) using a mass flow controller (Bronkhorst, UK). A high resolution camera connected to a computer was used to capture the foam height as a function of time at the defined time intervals. For experiments where the influence of oil was investigated, oil and surfactant solution were gently placed into the column before gas sparging began. We used a constant oil fraction of 5% (volume fraction relative to the surfactant solution) in all experiments. Each experiment was performed several times to ensure repeatability and consistency.

2.3. Bubble-scale foam stability

In addition to the bulk-scale experiments described above, foam stability was also studied at the bubble-scale. To do so, foam was injected into a Hele–Shaw cell made of two plexiglass plates with length and width of 25 cm and 15 cm, respectively. A gasket of thickness 0.03 cm was clamped in-between the two plates to create a small gap of size 0.03 cm (the gasket was incompressible). The gasket also provided a complete seal to prevent any leakage from the system. Fig. 1(b) shows the experimental setup. The foam dynamics and evolution at bubble-scale were recorded over time using an automated monochromic camera (Dalsa Genie TS-2500 which uses an advanced Teledyne DALSA CMOS monochrome sensor with

Table 2

Properties of oils used in our experiments to investigate foam stability in the presence of oil. The surface tension was measured at room temperature by the use of a tensiometer. The densities and viscosities were obtained from the supplier.

Oil	Hydrocarbon composition	Kinematic viscosity 25 °C (mm ² /s)	Density (g/cm ³)	Surface tension (mNm ⁻¹)
Isopar G	C10–C12	1.13	0.746	22.57
Isopar N	C12–C16	2.99	0.787	24.83
Isopar V	C14–C19	13.30	0.815	25.44

a resolution of 2560 × 2048) every 10 min controlled by a computer. A lightbox was placed underneath the system to enhance the illumination. The output images were 8-bit grayscale images with a spatial resolution of 19.4 pixels/mm.

The foam generator was constructed from a plexiglas column with an internal diameter and height of 4 cm and 10 cm respectively. Similar to the bulk-scale experimental setup, a sintered glass disk was fitted to the bottom of the column for gas sparging. Foam was generated in the reservoir by injecting air from the bottom using the mass flow controller under the same conditions described previously. When the cell was completely filled with foam, the injection was terminated and the foam evolution and dynamics were recorded using the camera mounted above the sample (as illustrated in Fig. 1(b)). Two series of experiments were conducted using this setup: (i) foam coarsening and the stability of the lamellae of all four surfactants were re-examined and the results were compared with the ones obtained from the bulk-scale experiments, and (ii) the effect of the oil on bubble coarsening and stability was also investigated. In the case of oil, both foam and oil were injected simultaneously into the Hele–Shaw cell. The oil was injected by the use of a syringe pump (Harvard Apparatus) at a rate 1.5 cm³/min such that the oil mixed with the foam before entering the Hele–Shaw cell.

2.4. Image analysis

The images were segmented and analyzed using Image J software. Fig. 2 illustrates a typical grey-scale image recorded by the camera during the bubble-scale experiment with the corresponding black and white image. In addition, the bubble size distribution with the corresponding maps were determined by two standard plugins in Image J namely Analyse Particles and Particle Analyser. This process was applied to all images to delineate the evolution of foam in the Hele–Shaw cell at the bubble-scale.

3. Results and discussions

3.1. Foam stability in the absence of oil: bulk-scale experiments

After the column was filled to a height of 60 cm (±1 cm), the air sparging into the cylindrical foam column was terminated. Then foam height reduction was monitored over time. Fig. 3 shows the foam decay profiles of the four surfactants used in our experiments in the absence of oil measured from the images of the foam column.

In the bulk-scale experiments, the half-decay time (defined as the time taken to reach half of the initial height of the foam) was used as the criterion to quantify foam stability such that the higher the half-decay time the more stable the foam and vice versa. This criterion was used in several previous studies [30,46]. Our results show that the Triton X100 foam is the least stable foam with the half-decay time of 40 min and the Cocobetaine foam has the highest stability with the half-decay time of 450 min in the absence of oil. The half-decay times of the foams are later compared in Section 3.2.

Generally, ionic surfactants form more stable foams due the strength of electrostatic double layer effect resulting from charge interactions at the film interface [53]. This important effect is suppressed in non-ionic surfactants, which may be the primary reason for the very low stability recorded for Triton X100. Additionally, Myers [53] reports that foams generated by non-ionic surfactants are usually unstable as they have large surface area per unit molecule as a result of the nature of their solvation mechanism. Consequently, the adsorbed surfactant molecules do not interact sufficiently at the interface leading to a low interfacial elasticity. Other important aspects that improve foam stability such as the Gibbs–Marangoni effect is significantly low in non-ionic surfactant foams due to the size and nature of their head groups [53]. For example, in Triton X100, although the branched chain polyethylene oxide groups reduces the interfacial tension between the surfactant solution and oil (in an oil displacement context), it lowers the lateral chain interactions between the surfactant molecules resulting in a

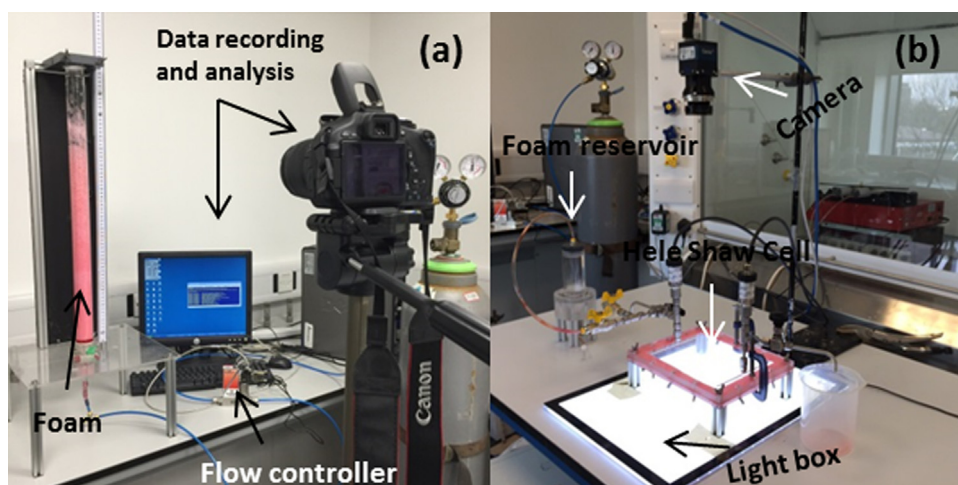


Fig. 1. (a) Experimental setup to investigate foam stability at bulk-scale showing the mass flow controller for air flow control and the camera to record height of foam over time. (b) 2D Hele–Shaw cell used to investigate foam stability at bubble-scale. The time evolution of the bubbles was captured by an automated high resolution monochromic camera and the dynamics of the foams were investigated from the images.

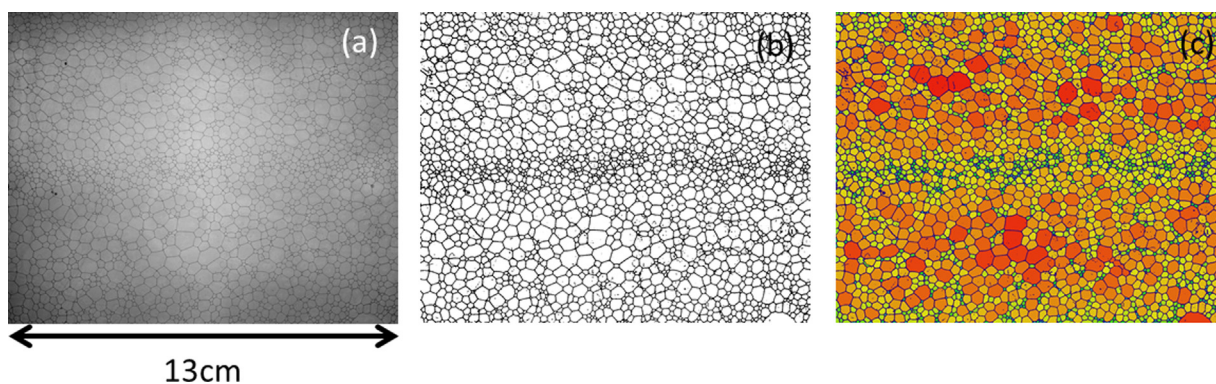


Fig. 2. A typical grey-scale image recorded by the monochromic camera (a) with the corresponding black and white image (b) indicating foam films (lamellae) and dispersed gas (or the area filled with air), respectively and (c) showing a color map of the bubble size distribution with color closer to red indicating a larger bubble. (For interpretation of the references to color in this figure legend, the reader is referred to the web version of this article.)

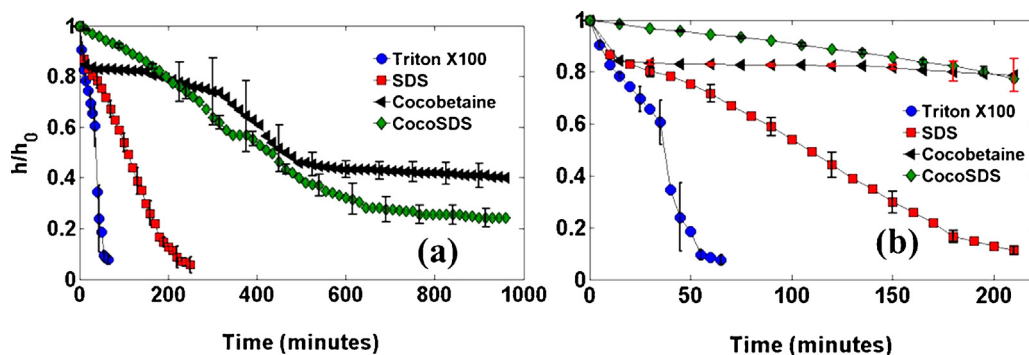


Fig. 3. (a) Height decay profile of foam (made from different surfactants presented in the legend) in the absence of oil. h and h_0 on the y-axis corresponds to the actual height and initial height of foam at the onset of the experiment, respectively. (b) Shows the decay profile of the various foams within the first 200 min of the experiments. The foam height was measured from the top of the foam to the top of the drained liquid in the foam column. The error bars indicate the standard deviation over 3 repeat measurements. Results show that the foam made by Cocobetaine is the most stable foam while Triton X100 is the least stable one.

reduced surface viscosity and film elasticity which leads to lower stability [53].

Based on Fig. 3, foam stability according to the half-decay times is ranked as the following Cocobetaine > CocoSDS > SDS > Triton X100. This result shows the significant effect of the type of the surfactant on the foam stability. Another factor that affects foam stability is liquid drainage. This phenomenon governs the primary phase of foam destabilisation. Fig. 3 shows that during the first 200 min CocoSDS is the most stable among the four surfactants. This is potentially due to the viscosity of the solution (please see Table A.1 in the Appendix A). The viscous nature of the surfactant solution results in slow drainage of liquid through the Plateau borders. To investigate further, the effect of drainage on the observed foam stability profiles and to delineate the contribution of liquid drainage to the overall stability of foams, subsequent experiments were conducted to measure liquid drainage with time. This was achieved by measuring the mass of the liquid that drained from the foam with an automated mass balance immediately after air sparging was terminated. In Fig. 4, the mass of the drained liquid is presented as a fraction of the mass of the total surfactant solution originally in the column prior to gas sparging.

Fig. 4 shows that liquid drainage was fastest in Triton X100. This is consistent with its shortest half-decay time and its least stability compared to the other surfactants used in this study. The order of stability was however reversed in the case of SDS and Cocobetaine for the drainage test. In other words, although the foam made by Cocobetaine was more stable than SDS (Fig. 3), the rate of liquid drainage from the foam in the primary decay stage was greater in Cocobetaine than SDS after a given time from the onset of the experiment as illustrated in Fig. 4. Hence, if one only considers the

drainage curves presented in Fig. 4, it may appear that the foam made by SDS is more stable than Cocobetaine; contrary to what was observed in Fig. 3. This shows there is not a perfect correlation between foam drainage and overall foam stability [54]. This issue can be explained using the images presented in Fig. 5 showing the liquid fraction of the foams after a certain elapsed time from the onset of the experiments. One can deduce from Fig. 5 that it is possible for foam to undergo rapid liquid drainage and still be more stable (the same phenomenon is observed in the case of Cocobetaine and CocoSDS where CocoSDS is initially more stable due to slow liquid drainage but eventually collapses before Cocobetaine i.e., Fig. 3).

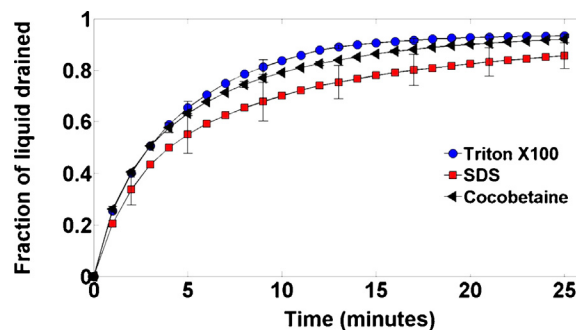


Fig. 4. Foam drainage curves over time for Triton X100, SDS and Cocobetaine. The error bars indicate the standard deviations. CocoSDS is not presented in this figure since the solution was too viscous (see Appendix A) to flow freely through the fine sintered disk confirming that the liquid drainage in CocoSDS was much slower.

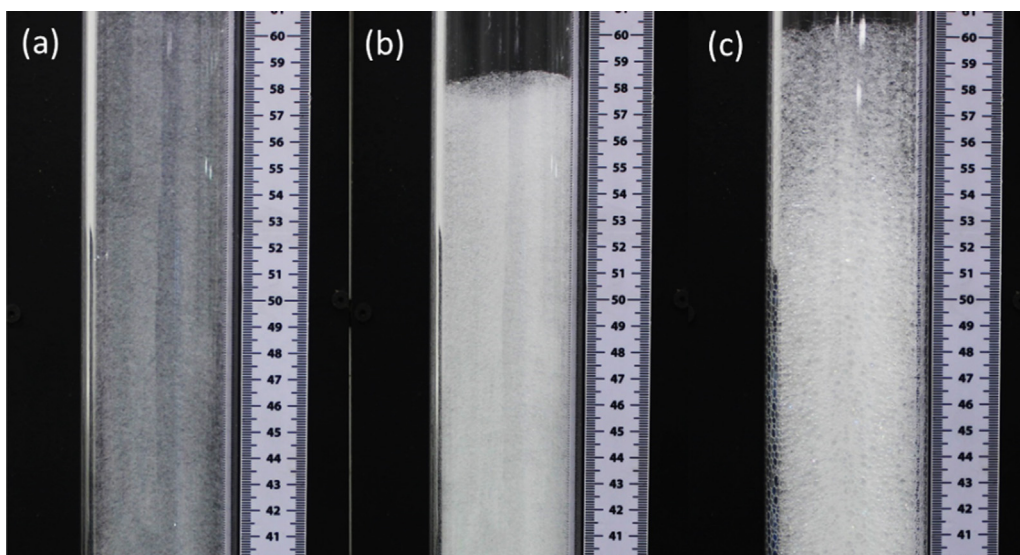


Fig. 5. The liquid fraction of foam (a) Cocobetaine (b) SDS, and (c) CocoSDS after 40 min from the onset of the drainage experiments. High intensity indicates less liquid drainage from the foam. The images confirm that the liquid drains much faster in the case of Cocobetaine (a) compared to SDS (b) after a given time from the onset of the experiment and that CocoSDS has more resistance to liquid drainage as well as height decay. Note that these images were taken in the bulk scale experiments where drained liquid stayed in the column (outlet was shut) hence no significant change in height for Cocobetaine and CocoSDS (i.e., they were more stable). In Fig. 3, the height of the drained liquid in the column was subtracted from the recorded height to obtain the actual height of the foam). The intensity of foam in the case of CocoSDS shows slight liquid drainage at the top, this is probably due to the fact that the bubbles created by this foam were relatively bigger than all the other foams [54] (the same is observed in the bubble-scale experiment explained in the following section, see Fig. 9). However, it took longer for this liquid to finally arrive at the bottom of the column.

Fig. 5(c) confirms that CocoSDS showed high resistance to liquid drainage as well as height decay as described earlier in Fig. 3. It is observed from Fig. 5 that Cocobetaine foam is much dryer than the SDS foam. This is due to the fact that during the initial stages of foam decay, there is rapid and uniform drainage of liquid from foam in Cocobetaine. Though it is likely that diffusive foam coarsening may be occurring during this period, bubble collapse does not occur simultaneously due to the stability of the foam films. On the contrary, the reduction in foam height in spite of slower liquid drainage rate in SDS suggests that bubbles are rupturing even during the first stage of foam decay. The foam is still wet according to the intensity of the foam in the image suggesting that the coarsening is occurring at a very slow rate in this foam. This explains the faster collapse time in the SDS foam compared to Cocobetaine foam (Fig. 4) even though more liquid has drained from the latter. Moreover, the Cocobetaine foam may have higher critical capillary pressure (which corresponds to a lower critical film thickness before rupture) compared to the SDS causing higher stability after rapid liquid drainage [41]. To summarize, the physicochemical properties of different surfactant foams influence foam drainage as well as the tolerance of the foams to capillary suction pressure and subsequently bubble collapse.

In any case, Figs. 3–5 show that considering only the decaying height of bulk foam over time (i.e., foam decay curve) may not provide the full picture about the evolution of the foam (stability and wetness) which is the common method used to investigate foam stability [39,46] because, as shown in the case of Cocobetaine, the foam may be quite stable in terms of its height but practically very dry as shown in Fig. 5 which may impact on foam stability and performance in the presence of mechanical oscillations as a result of foam displacement in porous media. Addressing this issue together with our interest to study foam stability at bubble-scale were the motivations to probe for an alternative method to further investigate foam stability and the information derived from the bulk-scale experiments. This alternative method will be discussed in Section 3.3 and 3.4.

3.2. Foam stability in the presence of oil: bulk-scale experiments

In Section 3.1, foam stability was investigated in the absence of oil. In this section, foam stability is investigated at the bulk-scale in the presence of oil. To do so, a comprehensive series of experiments were conducted to investigate the surfactants' ability to generate stable foams in the presence of different oils. Fig. 6 shows the foam decay profiles for different surfactants used in this study in the presence of Isopar G, Isopar N and Isopar V, with carbon chains lengths of C10–C12, C12–C16 and C14–C19, respectively. Fig. 6 confirms the destabilising effect of oil on foams compared to the case where oil was absent (comparing Figs. 3 and 6). Fig. 6 shows that increasing hydrocarbon chain length results in the formation of more stable foams. In other words, Isopar G consisting of the shortest chain hydrocarbons produced the highest destabilising effect on foam while the stability of the foams in the presence of Isopar V was the highest (particularly in the case of CocoSDS).

The influence of the type of oil on foam stability is further analyzed in the histogram of half-decay times of foams in the presence of various oils in Fig. 7. Our results are consistent with conclusions made in previous studies that lower chain hydrocarbons are detrimental to the foam stability [28–30,46]. The order of stability of the surfactants was changed in the presence of oil such that CocoSDS was the most stable in all three cases. The destabilizing effect of Isopar G was very pronounced in all the surfactants used in this study as presented in Fig. 7. In comparison to the case where oil was absent, the half-decay time was reduced by a factor of 11 in Cocobetaine and 6.5 in CocoSDS in the presence of 5% v/v of Isopar G. In the case of Cocobetaine, the thin films (resulting from rapid drainage of the liquid) may render the foam incapable of withstanding the spreading of comparatively low viscosity Isopar G consisting of smaller molecules hence the significant decline in the foam stability. For CocoSDS, spreading of Isopar G (see Section 3.2.1 and Table A.2) may have altered the surface elasticity as well as the surface viscosity of the foam suppressing the lamellae stability. The alterations of the surface properties could be caused by depletion of surfactant molecules at the gas-liquid interface due to oil displac-

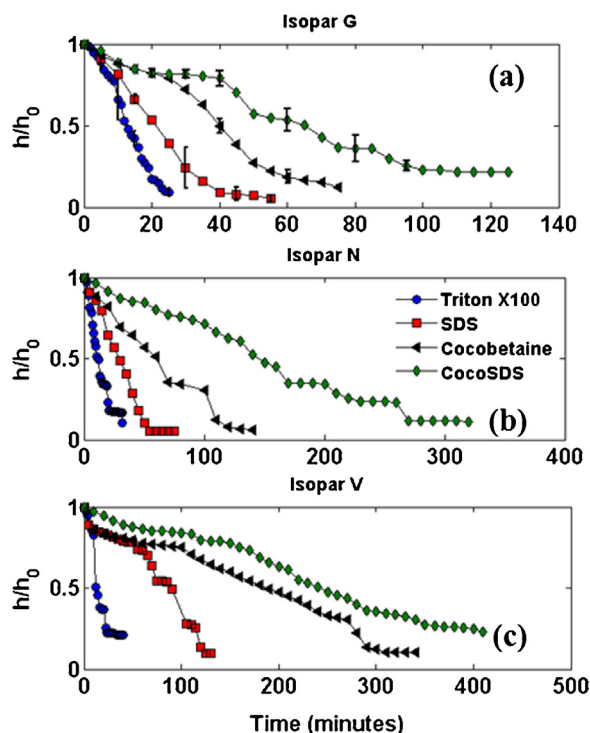


Fig. 6. Foam decay in the presence of (a) Isopar G (C10–12), (b) Isopar N (C12–16) and (c) Isopar V (C14–19). Oil fraction was 5% (v/v) of total surfactant solution in all cases. Results confirm that all three oils reduce foam stability. The longer the carbon chain length, the lesser the foam stability is reduced.

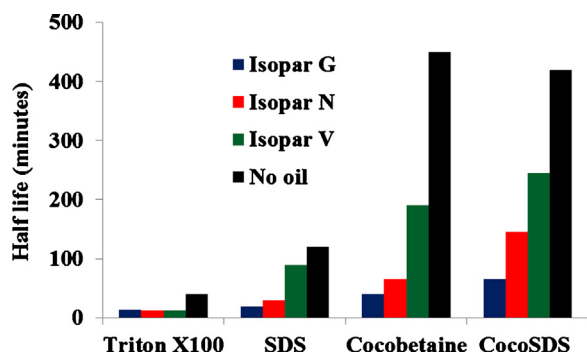


Fig. 7. The half-decay times of foams used in this study in the absence and presence of Isopar G, N and V determined from the bulk foam experiments. Results show that oils with lower viscosity and density induce a more destructive effect on foam stability.

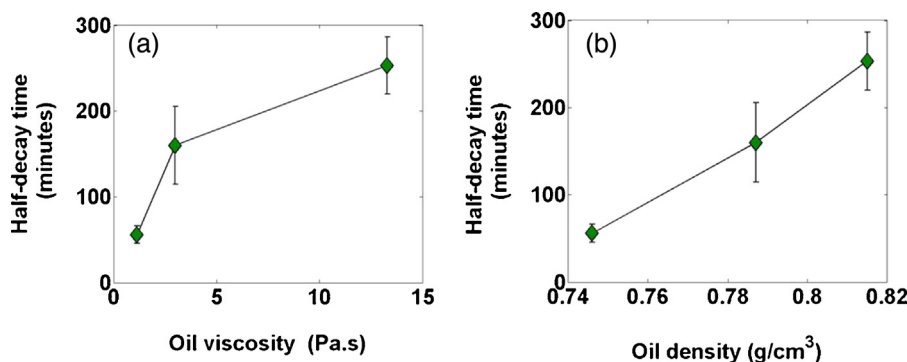


Fig. 8. (a) The effects of oil viscosity and (b) density on the half-decay time of foam made by CocoSDS surfactant. Results show that foam stability increases as oil density and viscosity increases.

Table 3

The entering, spreading and bridging coefficients of selected surfactants in the presence of Isopar N.

Surfactant	E (mN/m)	S (mN/m)
Triton X100	6.07	6.96
SDS	5.48	5.16
Cocobetaine	6.86	6.13
CocoSDS	2.51	3.90

ing or disrupting the surfactant molecules and their arrangement at the interface [53].

Short chain hydrocarbons have higher destabilizing effect on foams because they have smaller molecular elements which make it more probable for them to solubilize into the micelle aggregates. Lobo et al. [55] have shown that solubilization of oil in the micelles result in an increase in the van der Waals forces between the micelles. This leads to a decrease in micellar volume concentration and suppression in film stratification [31]. This in turn decreases foam stability. This trend can also be explained by the conclusion made by Hadjiiski et al. [56] regarding entry barrier reduction. In their experiments, they discovered that the entry barriers in the presence of a spread oil layer increased with increasing molecular mass of alkanes. Since molecular mass increases with increasing chain length for a given hydrocarbon series, the trend observed in our experiment may be attributed to this phenomenon. Besides, one may expect more dispersion of oil droplets in the bulk foam as viscosity and density of oil reduces. This may reduce foam stability as the contact between oil and foam network increases which eventually results in foam destabilization. The difficulty of droplets penetrating pseudoemulsion films is increased according to the changes in physiochemical properties of the oil as the chain length of the hydrocarbon increases. This is also visible in the case of Cocobetaine in the presence of Isopar V. The half-decay time is considerably closer to that of CocoSDS than in the case of Isopar G and Isopar N. Additionally, Fig. 7 shows that Triton X100 has very low tolerance to oil. Foam destruction in this case was so significant that its stability seemed indifferent to the type of oil added. The half-decay time in the presence of the three oils differed by only one minute in no particular order.

The experiment with CocoSDS foam was repeated several times to ensure the reproducibility of the data regarding the effects of oil viscosity and density on the foam stability. The results are presented in Fig. 8 confirming that the higher the viscosity and the density of the particular hydrocarbons used in our experiments, the more stable the CocoSDS foam. However, it must be added here that, since density contrast is comparatively small compared to the change in viscosity, the radical changes in half-decay time is probably influenced more by the viscosity of the oils.

3.2.1. Entering and spreading co-efficient

In this section, we compare and relate the results obtained from the bulk-scale foam experiments to the entering, spreading and bridging coefficients which are employed in the classical theory used to predict foam stability. It is noteworthy that though values of these coefficients may give insight as to the possibility of oil destroying foam, they do not determine the rate of foam destabilization [40,41]. Table 3 presents the entering, spreading and bridging coefficient for all surfactants in the presence of Isopar N (see Appendix A for Isopar G and V). All the surfactants recorded a positive entry coefficient indicating that oil entry is feasible in all

systems hence we have discussed the foam stability by the magnitude of the spreading coefficients (bridging co-efficient is irrelevant as all the spreading coefficients are positive). Triton X100 recorded the highest spreading coefficient which is consistent with its lowest stability. Additionally, CocoSDS had the lowest spreading coefficient in the presence of Isopar G, N and V which aligns with its highest stability in the presence of all three oils. SDS should be more stable than Cocobetaine given that it has a lower spreading coefficient; however this was not observed in the bulk foam experiment. This analysis shows that the overall foam stability is not dictated solely by these thermodynamic coefficients and it is also

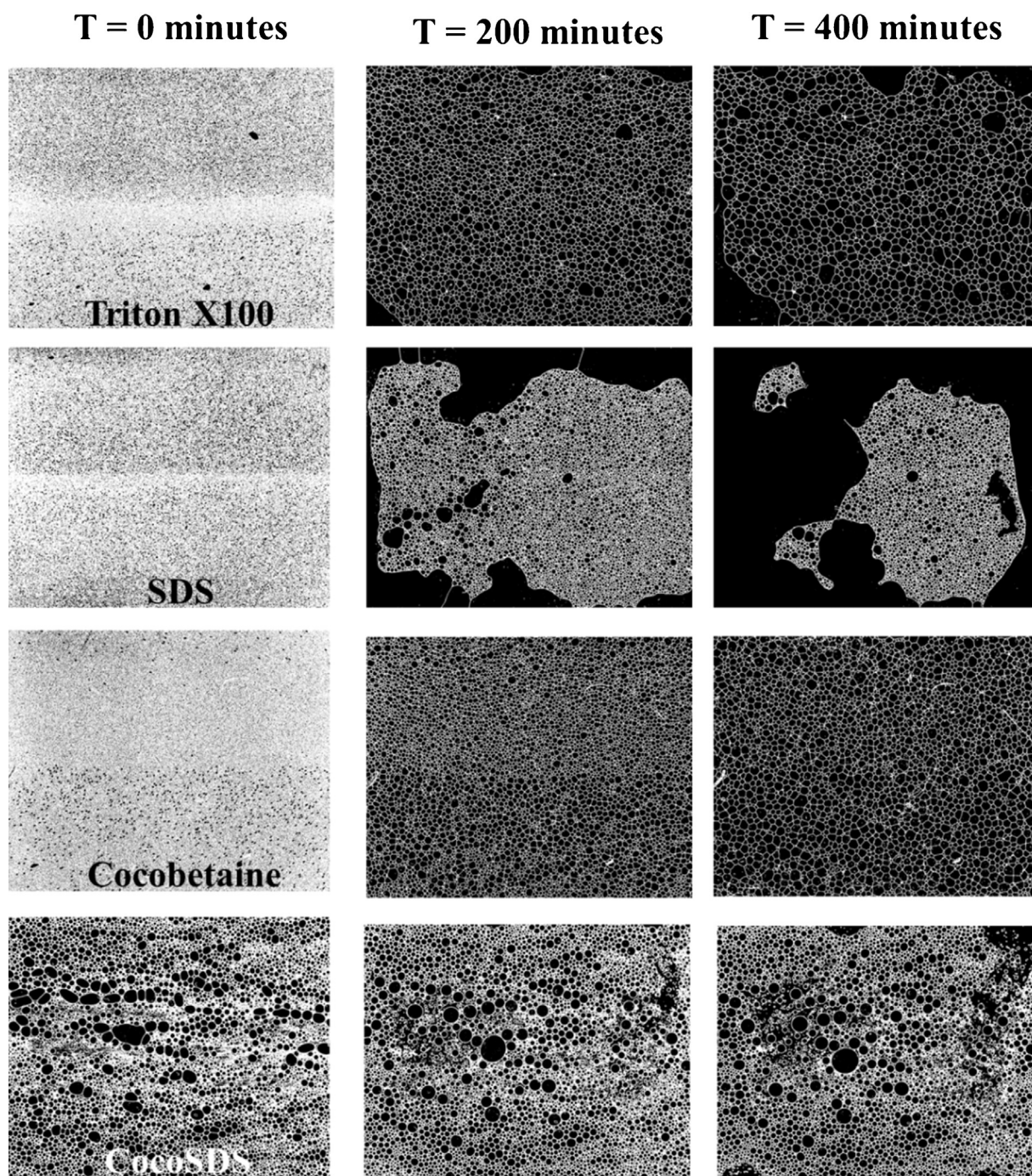


Fig. 9. Foam patterns and evolutions of four surfactants used in this study at different times from the onset of the experiments. The Hele–Shaw cell was placed horizontally. Images show the degree of coarsening and destruction in the foams as influenced by the type of surfactant. The white color in the image represents the lamellae while the black represents the air phase. The figure shows that SDS undergoes major destruction while CocoSDS shows little coarsening.

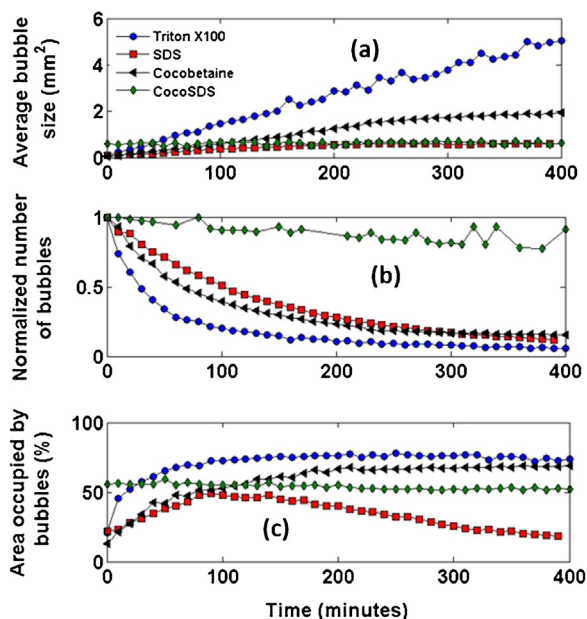


Fig. 10. (a) Average bubble size, (b) normalized number of bubble (number of bubble at each point normalized by the initial number of bubbles) and (c) the area occupied by bubbles (apparent area occupied by gas in foam relative to the area of the Hele–Shaw cell) calculated from the black and white images of the four surfactants used in our experiments. In general, Triton X100 shows the lowest stability to foam coarsening while SDS has lowest stability against bubble rupture as indicated in (c).

related to the interfacial and bulk properties of the surfactant and the strength of the entry barrier at the gas liquid interface [41].

3.3. Foam stability in the absence of oil: bubble-scale

In this section, foam stability is investigated against coarsening and rupture which together with the liquid drainage influence foam stability. A series of experiments were conducted using a transparent 2D Hele–Shaw cell described in Section 2.3 using the setup shown in Fig. 1(b). In the 2D foam experiments, the dominant contribution to foam destruction is coarsening (by gas diffusion and/or coalescence) since the effect of gravity is essentially negligible (the Hele–Shaw cell was placed horizontally and the gap between the glass plates was only 0.03 cm). As mentioned previously, the camera resolution was 19.4 pixels/mm. In the image analysis, the cut off bubble size was set to 0.02 cm² such that any closed object with a size lower than that was disregarded. Fig. 9 shows qualitatively the state of the foams in the Hele–Shaw cell at different times from the onset of the experiments for the four surfactants used in this study.

Using the segmented black and white images, the average bubble size, the number of bubbles and the area occupied by the gas in the Hele–Shaw cell (including only gas in the foam bubbles) was determined as a function of time to quantify the dynamics and characteristics of foams at bubble-scale (Fig. 10). The bubble size of CocoSDS foam was initially the coarsest. This effect was probably as a result of the viscosity of the surfactant solution (during the test, it took longer for bubbles to break out into the solution as the gas was being injected in CocoSDS. This was not seen in the other surfactants). It was observed in general that all foams coarsened over the course of the experiment; however it was almost negligible in the case of CocoSDS as the state of the foam in the Hele Shaw cell after 400 min was almost the same as in the beginning of the experiment. This is further supported by Fig. 10(a) and (c) showing a nearly constant value for the average bubble size as well as area occupied by the gas in CocoSDS foam over time. The reason for this high stability could be attributed to the thickness of the

lamella created by the foam as a result of high viscosity of the solution. Therefore, since foam drainage and the strong Plateau border suction it induces are absent in this case (horizontal cell), the thick lamellae are able to withstand inter-bubble gas diffusion.

Triton X100 recorded the highest coarsening rate of the four surfactants as evidenced by Fig. 10. The average bubble size after 400 min was about 5, 2, 0.6 and 0.6 mm² in the case of Triton X100, Cocobetaine, SDS and CocoSDS, respectively. Additionally, Fig. 10(b) shows that the time taken for the number of bubbles to reduce to half of its original value is much lower for Triton X100 (30 min) than for the rest of the surfactants (68 min for Cocobetaine and 100 min for SDS).

Fig. 10(a) and (b) alone do not provide us with complete information about the SDS stability compared to Cocobetaine. Because, while according to Fig. 10(a) and (b) the stability of the former against coarsening may be higher, its stability against rupture of the bubbles is much lower based on the information presented in Figs. 9 and 10(c). This may support the conclusion made in the bulk-scale tests that bubbles made with SDS rupture and collapse long before the liquid drains and the films thin.

The degree of coarsening can also be determined qualitatively from the bubble size distribution over time. Fig. 11 shows the bubble size distribution for the three surfactants from the beginning of the experiments ($T=0$) and after 50 min and 350 min from the onset of the experiments. All three surfactant foams initially possess similar bubble size distributions. In Triton X100 and SDS, 83% and 81% (respectively) of the bubbles with area between 0.02 mm² and 0.52 mm² while Cocobetaine has 95% of bubbles within this size range (Fig. 11 (a), (d) and (g), respectively). After 50 min, Triton X100 undergoes significant coarsening (Fig. 11(b)) such that only about 50% of the remaining bubbles possessed bubble area within 0.02–0.52 mm² size range. This is significantly smaller than SDS (88%) and Cocobetaine (80%) foams after the same elapsed time. By considering the histograms of the three foams after 350 min, the order of coarsening could be expressed as follows – Triton X100 > Cocobetaine > SDS. Fig. 11 shows that after 350 min the foam made by Triton X100 has bubble sizes spread over a wider range such that only about 15% of the bubbles are within the first bin size whereas in the case of SDS about 55% of the bubbles still possessed bubble size between 0.02 and 0.52 mm².

3.4. Foam stability in the presence of oil: bubble-scale results

As indicated previously, the decay of height of foam at bulk-scale alone offers limited insights regarding the liquid fraction of the foam over time. The bulk-scale experiment to delineate foam stability may have another limitation in the presence of oil. For example, Fig. B.1 in Appendix B presents the structure of Cocobetaine foam observed during the bulk-scale experiment. It was observed that the oil randomly created big voids in the interior of the foam. This significant destruction of foam in the presence of oil (Isopar N in this case) made it almost impossible to define foam height accurately as the top of the foam would no longer be representative of the total foam height.

Using the bubble scale setup described in Fig. 1(b) the behavior of foam in the presence of oil was investigated. In this series of experiments, oil was injected simultaneously with foam into the Hele–Shaw cell until it was completely filled with the oil-foam mixture. We selected Cocobetaine surfactant to conduct these experiments. The results displayed in Fig. 12 demonstrate that the destabilizing effect of oil increases as the oil viscosity and density decreases.

This is in agreement with the results obtained in the bulk-scale foam experiments. When oil is present (for all three oils used in our experiments), initially the coarsening rate is high such that less viscous oil results in a higher coarsening rate (i.e., the slope of the line

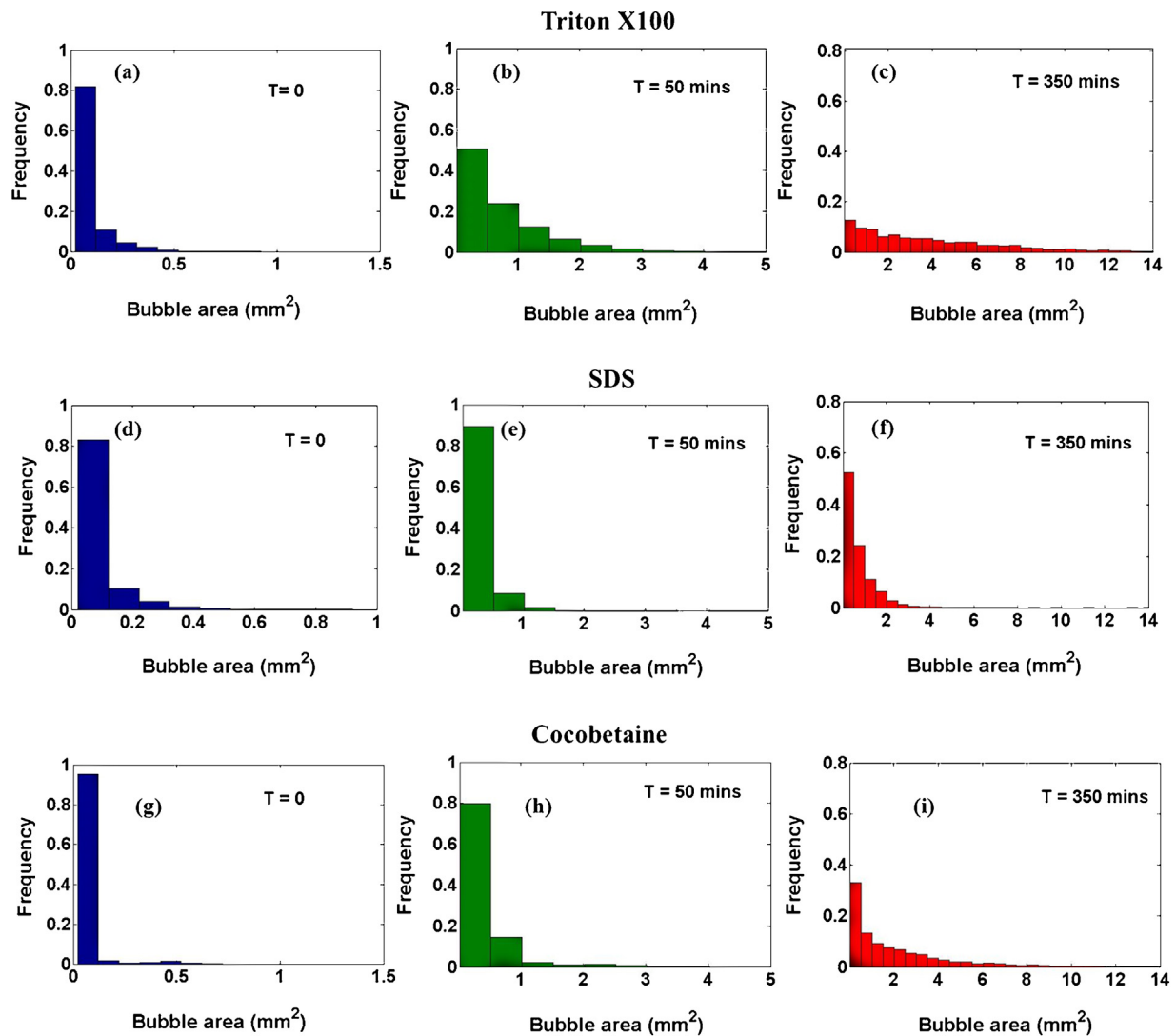


Fig. 11. Histograms of bubble size distribution of Triton X100 in (a)–(c), SDS in (d)–(f) and Cocobetaine in (g)–(i) at Time 0, 50 min and 350 min from the onset of the experiments, respectively. The frequency is expressed as the fraction of number of bubbles in a given bin size over the total number of bubbles.

at the initial stages depicted in Fig. 12). However, in our tests, after about 150 min, foam coarsening rate reached a plateau in all cases making foam stable. Our results show that as foam coarsens in the presence of oil, the bubbles became spherical rather than polyhedral as in the case of Cocobetaine in the absence of oil (compare Cocobetaine in Fig. 9 to Fig 13(d), (e) and (f)). This is responsible for the stability of the foams in the presence of oil after 150 min.

According to Fig. 12, one can deduce that the destabilizing effect of oil at the bubble-scale is not as pronounced as the one observed in the bulk-scale experiments. For example, Isopar G had a significant effect on Cocobetaine stability in the bulk-scale test reducing the half decay time from 450 min to 40 min while in the bubble-scale experiments, the time taken for number of bubbles to halve was reduced from 68 min to 28 min.

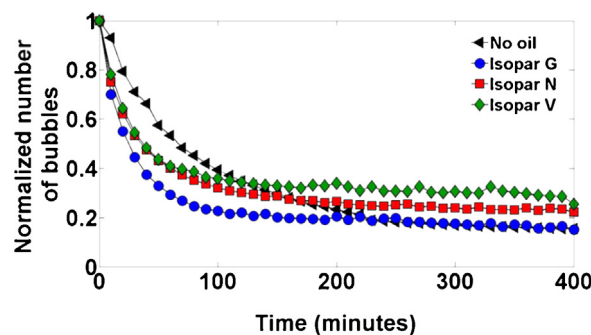


Fig. 12. The normalized number of bubbles in Hele–Shaw cell in the presence of Isopar G (C10–12), Isopar N (C12–16) and Isopar V (C14–19).

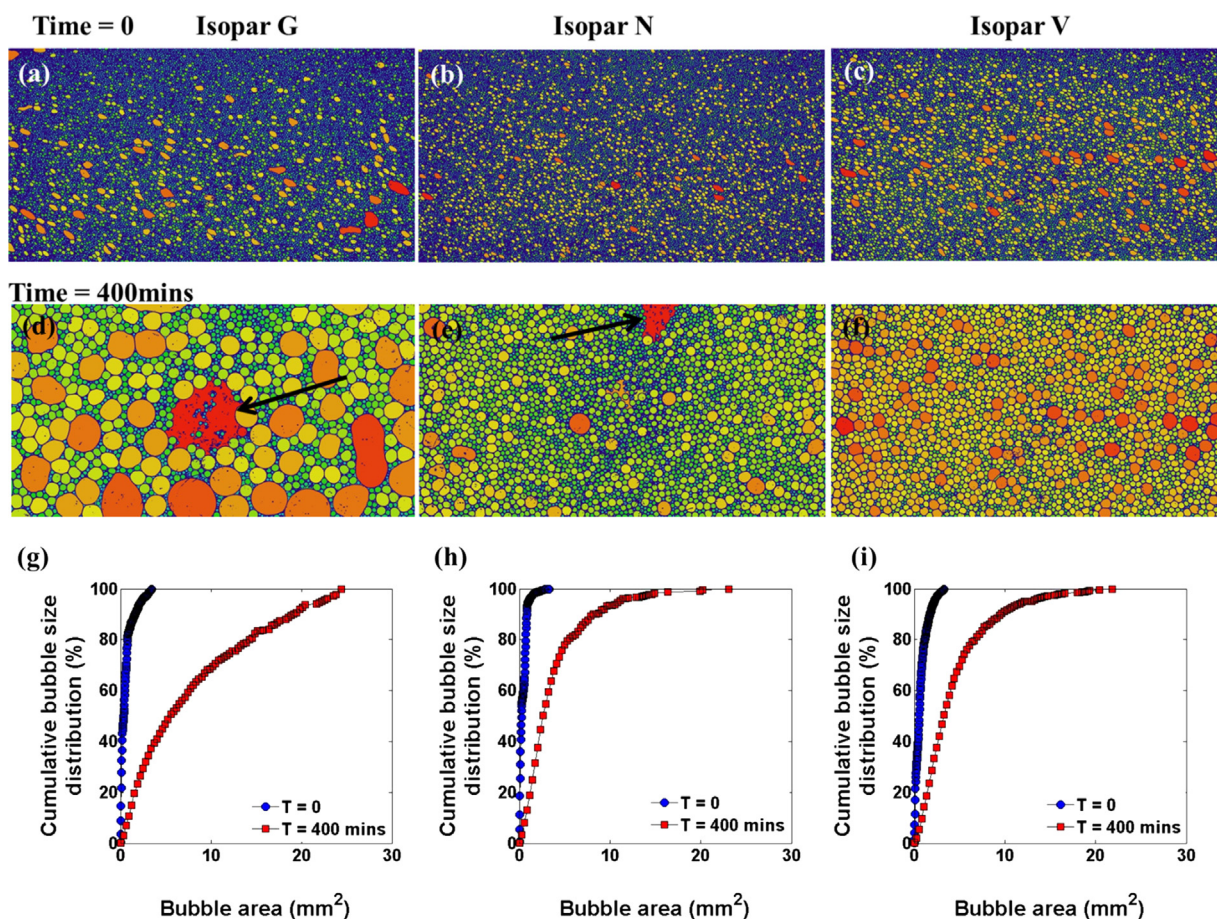


Fig. 13. Bubble size distribution in the presence of Isopar G (a), Isopar N (b) and Isopar V (c). Top and middle row show bubble size map at $T=0$ min (a–c) and $T=400$ min (d–f), respectively. The areas pointed by the arrow show oil-surfactant mixture as a result of oil destroying foam. Blue and red in the color size distribution represent small and big bubbles, respectively. The graphs (g–i) show the cumulative bubble size distribution of bubble area at the onset ($T=0$) and end ($T=400$ min) of the experiments. (For interpretation of the references to color in this figure legend, the reader is referred to the web version of this article.)

Fig. 13(a–f) displays visually the distribution of bubble sizes for Cocobetaine in the presence of oil at the bubble-scale at the beginning and the end of the tests. The effect of Isopar G is well pronounced in Fig. 13(d) as we observe a blob containing a mixture of oil and surfactant bigger than the biggest bubble in the Hele–Shaw cell after 400 min. In the presence of Isopar G, foam bubble size increases much more compared to Isopar N and V. The same phenomenon is observed quantitatively in Fig. 13(g–i) illustrating the bubble size distribution at the start (Time=0) and the end (Time = 400 min) of experiments.

4. Summary and conclusions

We have presented an investigation of foam stability of selected surfactants (cocamidopropyl betaine, sodium dodecyl sulphate, Triton X100 and CocoSDS made by mixing 1:1 ratio of cocamidopropyl betaine and sodium dodecyl sulphate) in the absence and presence of 3 isoparaffin oils with well-defined properties at bulk and bubble-scale. In the absence of oil, cocobetaine was the most stable at bulk-scale while CocoSDS (the surfactant mixture) demonstrated the highest stability in the presence of oil. The stability of the mixture is due to the presence of betaine in the mixture which potentially increased the critical capillary pressure of the foam films [43]. The high viscosity of CocoSDS compared to the other surfactants may also have influenced its stability by slowing down liquid drainage from the Plateau borders and consequently causing high resistance to film thinning. Our results clearly show that faster liquid drainage in foams does not necessarily correspond

to an overall low stability as it is possible for liquid to drain quickly from Plateau borders while thin lamellae remain stable. Also, as illustrated in Figs. 4 and 5, foam may be very stable in terms of its height even though it has drained to a small liquid fraction.

Besides, our results show that foam stability in the presence of oil largely depends on the surfactant type and oil properties. Small chain hydrocarbons with lower density and viscosity are more detrimental to the longevity of foams than long chain hydrocarbons.

At the bubble-scale, CocoSDS demonstrated the highest stability due to its bulk viscosity. The lamellae and the Plateau borders created by this surfactant combination were believed to be thicker than the other surfactants which improved its ability to withstand inter-bubble diffusion [57]. Our results show that the presence of oil increases coarsening rate of foams accordingly depending on the viscosity and density such that Isopar G with the lowest viscosity resulted in highest coarsening rate. Using the information obtained from the bubble-scale experiments, we have demonstrated that the coarsening rate of foams is reflected in the time evolution of the bubble size distribution of foams. This study suggests that a combination of bulk-scale and bubble-scale experiments is necessary to delineate adequately various facets of the physical phenomena that control the stability of foams.

Acknowledgments

Nima Shokri would like to acknowledge the donors of the American Chemical Society Petroleum Research Fund for partial support

of this research (PRF No. 52054-DNI6) and the equipment funding from The Royal Society (RG140088). Paul Grassia acknowledges sabbatical stay funding CONICET Argentina res. no.2218/13 and CONICYT Chile (folio 80140040). We would like to acknowledge the UK Engineering and Physical Sciences Research Council (EPSRC) to provide the PhD studentship (EP/L504877/1) for Kofi Osei-Bonsu. We would like to thank Prof. Bernie Binks at University of Hull for allowing us to use their instrument to measure interfacial tensions in our experiments and Mr. Craig Shore, Ian Small and Mr. Andrew Evans for their assistance with the experimental setup.

Appendix A.

Some of the physical properties of our systems are presented here. Table A.1 presents the viscosity data whereas

Table A.1

Viscosity of surfactant solutions at 2% concentration at different shear rates at 25 °C.

Surfactant	Viscosity (Pa s)	Viscosity (Pa s)	Viscosity (Pa s)
	0.1 (1/s)	1 (1/s)	10 (1/s)
Triton X100	0.10	7.74×10^{-3}	8.14×10^{-4}
SDS	0.09	3.52×10^{-3}	9.35×10^{-4}
Cocobetaine	0.09	1.78×10^{-3}	8.19×10^{-4}
CocoSDS	0.72	0.41	0.35

Tables A.2 and A.3 present the entering and spreading coefficients.

Table A.2

Entering, spreading and bridging coefficient in the presence of Isopar G. Entering, spreading and bridging coefficient has been defined in Eqs. (1)–(3).

Surfactant	E (mN/m)	S (mN/m)
Triton X100	8.01	6.75
SDS	7.12	5.26
Cocobetaine	9.61	5.11
CocoSDS	4.31	3.83

Table A.3

Entering, spreading and bridging coefficients of the surfactant solutions in the presence of Isopar V.

Surfactant	E (mN/m)	S (mN/m)
Triton X100	7.81	4.08
SDS	6.69	2.82
Cocobetaine	7.82	4.03
CocoSDS	1.31	1.09

Appendix B.

Fig. B.1 shows some of the challenges of measuring foam height in a bubble scale experiment.



Fig. B.1. Non-uniformed breakdown of foam made with Cocobetaine in the presence of Isopar N. This image highlights one of the major challenges in quantifying foam height in the bulk-scale experiment. The foam in the column is no longer representative of the true foam height. Although the data obtained from this image was not included in the analysis, this phenomenon occurred multiple times and posed a difficulty in quantifying the foam height accurately.

References

- [1] D. Green, G. Willhite, Enhanced Oil Recovery SPE Textbook Series, Richardson, TX, 1998, 2015.
- [2] M. Sahimi, Flow and transport in porous media and fractured rock: from classical methods to modern approaches, John Wiley & Sons, 2012.
- [3] W.R. Rossen, C.J. van Duijn, Gravity segregation in steady-state horizontal flow in homogeneous reservoirs, *J. Petrol. Sci. Eng.* 43 (2004) 99–111.
- [4] D.L. Kuehne, D.I. Ehman, A.S. Emanuel, C.F. Magnani, Design and evaluation of a nitrogen-foam field trial, *J. Petrol. Technol.* 42 (1990) 504–512.
- [5] Y.-B. Chang, M. Lim, G. Pope, K. Sepehrnoori, CO₂ flow patterns under multiphase flow: heterogeneous field-scale conditions, *SPE Reservoir Eng.* 9 (1994) 208–216.
- [6] A. Rashid, K. Liu, T. Sayem, A. Honari, M.B. Clennell, A. Saedi, X. Wei, Laboratory investigation of factors affecting CO₂ enhanced oil and gas recovery, in: In SPE Enhanced Oil Recovery Conference, Kuala Lumpur, Malaysia, 2013, SPE-165270.
- [7] D.J. Stephenson, A.G. Graham, R.W. Luning, Mobility control experience in the Joffre Viking miscible CO₂ flood, *SPE Reservoir Eng.* 8 (1993) 183–188.
- [8] A. Turta, A. Singhal, Field foam applications in enhanced oil recovery projects: screening and design aspects, *J. Can. Petrol. Technol.* 41 (2002).
- [9] A.R. Kovscek, C.J. Radke, Fundamentals of foam transport in porous media, in: L.L. Schramm (Ed.), *Foams: Fundamentals and Applications in the Petroleum Industry*, American Chemical Society, 1994, 2015, pp. 115–163.
- [10] R. Farajzadeh, A. Andrianov, H. Bruining, P.L. Zitha, Comparative Study of CO₂ and N₂ foams in porous media at low and high pressure-temperatures, *Ind. Eng. Chem. Res.* 48 (2009) 4542–4552.
- [11] G. Hirasaki, The steam-foam process, *J. Petrol. Technol.* 41 (1989) 449–456.
- [12] K. Ma, R. Lontas, C.A. Conn, G.J. Hirasaki, S.L. Biswal, Visualization of improved sweep with foam in heterogeneous porous media using microfluidics, *Soft Matter* 8 (2012) 10669–10675.
- [13] C. Zhang, M. Oostrom, J.W. Grate, T.W. Wietsma, M.G. Warner, Liquid CO₂ displacement of water in a dual-permeability pore network micromodel, *Environ. Sci. Technol.* 45 (2011) 7581–7588.
- [14] R. Farajzadeh, A. Andrianov, R. Krastev, G.J. Hirasaki, W.R. Rossen, Foam-oil interaction in porous media: implications for foam assisted enhanced oil recovery, *Adv. Colloid Interface Sci.* 183–184 (2012) 1–13.
- [15] G. Hirasaki, J. Lawson, Mechanisms of foam flow in porous media: apparent viscosity in smooth capillaries, *SPE J.* 25 (1985) 176–190.
- [16] A.H. Falls, G.J. Hirasaki, T.W. Patzek, D.A. Gauglitz, D.D. Miller, T. Ratulowski, Development of a mechanistic foam simulator: the population balance and generation by snap-off, *SPE Reservoir Eng.* 3 (1988) 884–892.
- [17] P. Grassia, E. Mas-Hernández, N. Shokri, S.J. Cox, G. Mishuris, W.R. Rossen, Analysis of a model for foam improved oil recovery, *J. Fluid Mech.* 751 (2014) 346–405.

- [18] R. Farajzadeh, A. Andrianov, P. Zitha, Investigation of immiscible and miscible foam for enhancing oil recovery, *Ind. Eng. Chem. Res.* 49 (2009) 1910–1919.
- [19] L.L. Schramm, F. Wassmuth, in: L.L. Schramm (Ed.), *Foams: Basic Principles, Foams: Fundamentals and Applications in the Petroleum Industry*, ACS, 1994, 2015, pp. 3–45.
- [20] E.J.W. Verwey, J.T.G. Overbeek, K. Van Nes, *Theory of the Stability of Lyophobic Colloids: the Interaction of Sol Particles Having an Electric Double Layer*, Elsevier New York, 1948.
- [21] B. Derjaguin, L. Landau, The theory of stability of highly charged lyophobic sols and coalescence of highly charged particles in electrolyte solutions, *Acta Physicochim. URSS* 14 (1941) 633–652.
- [22] A. Nikolov, D. Wasan, D. Huang, D. Edwards, The effect of oil on foam stability: mechanisms and implications for oil displacement by foam in porous media, in: *In SPE Annual Technical Conference and Exhibition*, San Antonio, Texas, 1986, SPE 15443.
- [23] L. Minssieux, Oil displacement by foams in relation to their physical properties in porous media, *J. Petrol. Technol.* 26 (1974) 100–108.
- [24] L.L. Schramm, J.J. Novosad, The destabilization of foams for improved oil recovery by crude oils: effect of the nature of the oil, *J. Petrol. Sci. Eng.* 7 (1992) 77–90.
- [25] N.D. Denkov, Mechanisms of foam destruction by oil-based antifoams, *Langmuir* 20 (2004) 9463–9505.
- [26] K. Mannhardt, J. Novosad, L. Schramm, Foam/oil interactions at reservoir conditions, in: *In Symposium on improved oil recovery*, Tulsa, Oklahoma, 1998, SPE 39681.
- [27] K. Mannhardt, I. Svorstøl, Effect of oil saturation on foam propagation in Snorre reservoir core, *J. Petrol. Sci. Eng.* 23 (1999) 189–200.
- [28] A. Andrianov, R. Farajzadeh, M. Mahmoodi Nick, M. Talanana, P.L.J. Zitha, Immiscible foam for enhancing oil recovery: bulk and porous media experiments, *Ind. Eng. Chem. Res.* 51 (2012) 2214–2226.
- [29] F. Suffridge, K. Raterman, G. Russell, Foam performance under reservoir conditions, in: *In SPE Annual Technical Conference and Exhibition*, San Antonio, Texas, 1989, SPE-19691.
- [30] R. Aveyard, B.P. Binks, P.D.I. Fletcher, T.G. Peck, C.E. Rutherford, Aspects of aqueous foam stability in the presence of hydrocarbon oils and solid particles, *Adv. Colloid Interface Sci.* 48 (1994) 93–120.
- [31] K. Koczko, L.A. Lobo, D.T. Wasan, Effect of oil on foam stability: aqueous foams stabilized by emulsions, *J. Colloid Interface Sci.* 150 (1992) 492–506.
- [32] W.D. Harkins, A general thermodynamic theory of the spreading of liquids to form duplex films and of liquids or solids to form monolayers, *J. Chem. Phys.* 9 (1941) 552–568.
- [33] J.V. Robinson, W.W. Woods, A method of selecting foam inhibitors, *J. Soc. Chem. Ind.* 67 (1948) 361–365.
- [34] H.C. Lau, S.M. O'Brien, Effects of spreading and nonspreading oils on foam propagation through porous media, *SPE Reservoir Eng.* 3 (1988) 893–896, SPE-15668.
- [35] P.R. Garrett, *The Science of Defoaming: Theory, Experiment and Applications*, CRC Press, 2013.
- [36] D. Vitasari, P. Grassia, P. Martin, Surfactant transport onto a foam lamella, *Chem. Eng. Sci.* 102 (2013) 405–423.
- [37] W. Ewers, K. Sutherland, The role of surface transport in the stability and breakdown of foams, *Aust. J. Chem.* 5 (1952) 697–710.
- [38] K. Koczko, J.K. Koczko, D.T. Wasan, Mechanisms for antifoaming action in aqueous systems by hydrophobic particles and insoluble liquids, *J. Colloid Interface Sci.* 166 (1994) 225–238.
- [39] A.K. Vikingstad, A. Skauge, H. Høiland, M. Arra, Foam–oil interactions analyzed by static foam tests, *Colloid Surf. A* 260 (2005) 189–198.
- [40] D.J. Manlowe, C.J. Radke, A pore-level investigation of foam/oil interactions in porous media, *SPE Reservoir Eng.* 5 (1990) 495–502.
- [41] A. Hadjiiski, N.D. Denkov, S. Tcholakova, I.B. Ivanov, Role of entry barriers in the foam destruction by oil drops, in: K.L. Mittal, D.O. Shah (Eds.), *Adsorption and Aggregation of Surfactants in Solution*, Marcel Dekker, New York, 2003, pp. 465–498.
- [42] R.F. Li, G.J. Hirasaki, C.A. Miller, S.K. Masalmeh, Wettability alteration and foam mobility control in a layered 2-D heterogeneous system, in: *In SPE International Symposium on Oilfield Chemistry*, The Woodlands, Texas, 2011, SPE-141462.
- [43] E.S. Basheva, D. Ganchev, N.D. Denkov, K. Kasuga, N. Satoh, K. Tsujii, Role of betaine as foam booster in the presence of silicone oil drops, *Langmuir* 16 (1999) 1000–1013.
- [44] T. Blaker, M.G. Arra, A. Skauge, L. Rasmussen, H.K. Celius, H.A. Martinsen, F. Vassenden, Foam for gas mobility control in the Snorre field: the FAWAG project, in: *In SPE Reservoir Evaluation Eng.*, Houston, Texas, 2002, SPE-56478.
- [45] Y. Zhang, X. Yue, J. Dong, L. Yu, New and effective foam flooding to recover oil in heterogeneous reservoir, in: *In SPE/DOE Improved Oil Recovery Symposium*, Tulsa, Oklahoma, 2000, SPE-59367.
- [46] M. Simjoo, T. Rezaei, A. Andrianov, P.L.J. Zitha, Foam stability in the presence of oil: effect of surfactant concentration and oil type, *Colloid Surf. A* 438 (2013).
- [47] S.A. Farzaneh, M. Sohrabi, Experimental investigation of CO₂-foam stability improvement by alkaline in the presence of crude oil, *Chem. Eng. Res. Des.* 94 (2015) 375–389.
- [48] H. Caps, N. Vandewalle, G. Broze, Foaming dynamics in Hele–Shaw cells, *Phys. Rev. E* 73 (2006) 65301.
- [49] D.J. Durian, Foam mechanics at the bubble scale, *Phys. Rev. Lett.* 75 (1995) 4780–4783.
- [50] J. Marchalot, J. Lambert, I. Cantat, P. Tabeling, M.-C. Jullien, 2D foam coarsening in a microfluidic system, *EPL (Europhys. Lett.)* 83 (2008) 64006.
- [51] M. Tong, K. Cole, S.J. Neethling, Drainage and stability of 2D foams: foam behaviour in vertical Hele–Shaw cells, *Colloids Surf. A: Physicochem. Eng. Aspects* 382 (2011) 42–49.
- [52] K. Lunkenheimer, K.-D. Wantke, Determination of the surface tension of surfactant solutions applying the method of Lecomte du Noüy (ring tensiometer), *Colloid Polym. Sci.* 259 (1981) 354–366.
- [53] D. Myers, *Surfactant Science and Technology*, John Wiley & Sons, New Jersey, 2005, pp. 253–261.
- [54] S. Hilgenfeldt, S.A. Koehler, H.A. Stone, Dynamics of coarsening foams: accelerated and self-limiting drainage, *Phys. Rev. Lett.* 86 (2001) 4704–4707.
- [55] L. Lobo, A. Nikolov, D. Wasan, Foam stability in the presence of oil: on the importance of the second virial coefficient, *J. Disper. Sci. Technol.* 10 (1989) 143–161.
- [56] A. Hadjiiski, S. Tcholakova, N.D. Denkov, P. Durbur, G. Broze, A. Mehreteab, Effect of oily additives on foamability and foam stability. 2. Entry barriers, *Langmuir* 17 (2001) 7011–7021.
- [57] D. Weaire, S. Hutzler, *The Physics of Foam*, Oxford University Press, 1999, pp. 89–101.